

Lead Leaching of Perovskite Solar Cells in Aqueous Environments: A Quantitative Investigation

Dong Yan, Xingwen Lu, Shiyi Zhao, Zuhong Zhang, Mingxia Lu, Jiangtao Feng, Jingchao Zhang, Kate Spencer, Trystan Watson, Meng Li,* Bo Hou,* Fei Wang,* and Zhe Li*

Lead halide perovskite solar cells (PSCs) have emerged as a highly promising next-generation photovoltaic (PV) technology that combines high device performance with ease of processing and low cost. However, the potential leaching of lead is recognized as a major environmental concern for their large-scale commercialization, especially for application areas with significant overlap with human life. Herein, a quantitative kinetic analysis of the Pb leaching behavior of five types of benchmark PSCs, namely, MAPbI₃, FA_{0.95}MA_{0.05}Pb(I_{0.95}Br_{0.05})₃, Cs_{0.05}(FA_{0.85}MA_{0.15})_{0.95}Pb(I_{0.85}Br_{0.15})₃, CsPbI₃, and CsPbI₂Br, under laboratory rainfall conditions is reported. Strikingly, over 60% of the Pb contained in the unencapsulated perovskite devices is leached within the first 120 s under rainfall exposure, suggesting that very rapid leaching of Pb can occur when indoor and outdoor PV devices are subject to physical damage or failed encapsulation. The initial Pb leaching rate is found to be strongly dependent on the types of PSCs, pointing to a potential route toward Pb leaching reduction through further optimization of their materials design. The findings offer kinetic insights into the Pb leaching behavior of PSCs upon aqueous exposure, highlighting the urgency to develop robust mitigation methods to avoid a potentially catastrophic impact on the environment for their large-scale deployment.


1. Introduction

Lead halide perovskite solar cells (PSCs) have emerged as a promising next-generation photovoltaic (PV) technology due to their material-related properties such as a high optical absorption coefficient, an optimal bandgap, excellent charge transport, and tolerance to defect, as well as advantages including ease of processing and low fabrication cost.^[1–7] Within just a few years of development, the power conversion efficiency (PCE) of PSCs reached over 25.7%, already comparable to established photovoltaic technologies such as crystalline silicon.^[8–12] With the rapid advances in materials and device design, PSCs have shown extraordinary potential for commercialization both as a standalone technology^[11] and in tandem with silicon photovoltaics^[13] for multiple application areas. The ability to deposit perovskite layers via multiple scalable techniques as well as the synthetic versatility for modulating transparency and color via composition

and crystal engineering allows PSCs to be an ideal solution for building-integrated photovoltaics and indoor photovoltaics.^[14,15]

D. Yan
Guangdong-Hong Kong-Macao Joint Laboratory for Intelligent Micro-Nano Optoelectronic Technology
School of Physics and Optoelectronic Engineering
Foshan University
Foshan 528225, P. R. China

D. Yan, M. Li, Z. Li
School of Engineering and Materials Science (SEMS)
Queen Mary University of London
London E1 4NS, UK
E-mail: mengli@qmul.ac.uk; zhe.li@qmul.ac.uk

 The ORCID identification number(s) for the author(s) of this article can be found under <https://doi.org/10.1002/solr.202200332>.

© 2022 The Authors. Solar RRL published by Wiley-VCH GmbH. This is an open access article under the terms of the Creative Commons Attribution License, which permits use, distribution and reproduction in any medium, provided the original work is properly cited.

DOI: 10.1002/solr.202200332

X. Lu
School of Environmental Science and Engineering, and Institute of Environmental Health and Pollution Control
Guangdong University of Technology
Guangzhou 510006, P. R. China

S. Zhao, F. Wang
School of Environment
Guangdong Key Laboratory of Environmental Pollution and Health
Jinan University
Guangzhou 510632, P. R. China
E-mail: wf1984@jnu.edu.cn

Z. Zhang, M. Li
Key Lab for Special Functional Materials of Ministry of Education National & Local Joint Engineering Research Center for High-efficiency Display and Lighting Technology
School of Materials Science and Engineering, and Collaborative Innovation Center of Nano Functional Materials and Applications
Henan University
Kaifeng 475004, P. R. China
E-mail: mengli@henu.edu.cn

Lead (Pb) plays a crucial role in the efficient operation of PSCs. Their ideal electronic configuration (e.g., Pb 6s lone-pair states and inactive Pb 6p orbital) and ionic radii are known as ideal divalent cations for perovskite light-absorbing materials.^[16] However, Pb is widely recognized as a harmful substance, which poses potential risks both to the natural and to the built environment.^[17] To minimize Pb content in PSCs, there has been increasing research effort in the development of Pb-free PSCs and PSCs with reduced Pb content, such as ASnX₃ tin perovskites, A₂B(I)B(III)X₆ double perovskites, and Sn/Pb mixed perovskites.^[18–20] However, the Pb-free alternatives typically possess a significantly lower PCE, attributed to their suboptimal optoelectronic properties such as nonideal bandgap and deep defects.^[21] Sn/Pb mixed PSCs possess reduced Pb content while still maintaining a relatively high PCE, but their stability decreases noticeably owing to the ready oxidation of Sn²⁺ to Sn⁴⁺.^[22–25] In addition to the research effort in full or partial Pb replacement, a number of Pb-containing methods have been explored to reduce the Pb leaching of PSCs through further optimization of their device architecture.^[26–32] For example, using Pb-absorbing or self-healing encapsulation materials, Pb leakage from damaged PSCs was significantly reduced without affecting the efficiencies of the cells.^[27–29] Huang et al. used the self-healing epoxy resin encapsulation and Pb-adsorbing ionogel-based encapsulation respectively, achieving simultaneous Pb leakage reduction and stability improvement of perovskite modules.^[27,29] Zhu et al. reported on-device sequestration of more than 96% of Pb leakage, achieved through Pb-absorbing coatings on both sides of PSCs.^[28]

Concerning the potential environmental impact of Pb-based PSCs, the leaching of Pb from PSCs upon aqueous exposure can be triggered by the degradation and decomposition of the perovskite materials, further accelerated by the accidental damage and disposal of PSCs.^[33,34] The leaked Pb can migrate in the environment and subsequently accumulate in living organisms via biouptake and human body via the food chain,^[17,35,36] known to be tenfold the mobility of other Pb compounds in daily human life.^[37] There has been increasing research effort in Pb leakage analyses and life cycle assessments of PSCs to understand their leaching process and evaluate their potential environmental impacts.^[17,36,38–41] Cahen et al. studied MAPbI₃ perovskite films exposed under aqueous environments with different pH values from 4.2 to 8.1 and found that the difference in Pb leaching amount is not significant.^[36] Nazeeruddin et al. demonstrated a two-stage dissolution process of Pb²⁺ ions from three different

types of PSCs (MAPbI₃, FA_{0.85}MA_{0.15}Pb(I_{0.85}Br_{0.15})₃, and Cs_x(MA_{0.17}FA_{0.83})_(100–x)Pb(I_{0.83}Br_{0.17})₃) and found that the amount of Pb leaching is within the same order of magnitude under simulated normal and acidic rainwater (pH = 5.6 and 4.5).^[39] Zhao et al. investigated the leaching concentrations of several heavy metals (e.g., Pb, Zn, Ni) in PSCs and confirmed that the Pb leaching amount surpasses the hazardous waste standard of 5 mg L⁻¹.^[38] Cheng et al. evaluated the potential Pb contamination of cracked perovskite modules under simulated working conditions and demonstrated that a widely used “sandwich” encapsulation strategy (utilizing polyolefin and polyisobutylene as encapsulants) could effectively prevent Pb leaching from perovskite modules.^[40] Among the abovementioned studies, only a few have conducted quantitative analysis of Pb leaching of PSCs. Furthermore, a comprehensive comparison of the kinetic Pb leaching behavior over a broad range of state-of-the-art PSCs is still lacking within the community.

In this work, we report a quantitative comprehensive analysis of the kinetic Pb leaching behavior based on five types of high-performance PSCs, namely, MAPbI₃, FA_{0.95}MA_{0.05}Pb(I_{0.95}Br_{0.05})₃ (abbreviated as FAMA), Cs_{0.05}(FA_{0.85}MA_{0.15})_{0.95}Pb(I_{0.85}Br_{0.15})₃ (abbreviated as FAMACs), CsPbI₃, and CsPbI₂Br, each optimized to PCEs comparable with values reported in the literature. Static soaking tests in acid solution were initially carried out to determine the total amount of Pb contained in each type of PSC, followed by kinetic leaching tests under various laboratory rainfall conditions. The kinetic leaching behavior, especially during the initial stages of Pb leaching, was revealed by measuring the Pb concentration of the residual solution at different time intervals. We observed that over 60% of the total amount of Pb was leached within the first 120 s of rainfall exposure of unencapsulated devices across all PSC samples studied, suggesting very fast Pb leaching kinetics. The initial leaching rates are found to be strongly dependent upon individual PSCs, indicating a material-dependent Pb leaching mechanism, although the difference in leaching rate is found to diminish over the longer term. A crosscomparison with PbS quantum dot solar cells, a promising next-generation PV technology based on another class of solution-processed Pb-based semiconductors, was also carried out, with similar Pb leaching rates observed. Our results provide quantitative kinetic insights into the Pb leaching kinetics of state-of-the-art PSCs, highlighting the importance and urgency to incorporate effective mitigation methods for Pb leaching toward their large-scale commercialization. Our findings also suggest that further optimization of the perovskite materials (guided by a comprehensive understanding of the materials parameters that control

M. Lu
School of Chemistry and Chemical Engineering
Henan University of Technology
Zhengzhou 450001, P. R. China

J. Feng
Department of Environmental Science and Engineering
Xi'an Jiaotong University
Xi'an 710049, P. R. China

J. Zhang
NVIDIA Corporation
Santa Clara, CA 95051, USA

K. Spencer
School of Geography
Queen Mary University of London
London E1 4NS, UK

T. Watson
SPECIFIC
College of Engineering
Swansea University, Bay Campus
Swansea SA1 8EN, UK

B. Hou
School of Physics and Astronomy
Cardiff University
Cardiff CF24 3AA, Wales, UK
E-mail: houb6@cardiff.ac.uk

the Pb leaching rate) could be a potential strategy toward reduction of Pb leaching, in addition to the existing effort in the development of Pb-free materials and device packaging and encapsulation approaches.

2. Results and Discussion

Water molecules can solvate (surface hydration with MAI or PbI) and infiltrate to interact with the Pb atoms, resulting in the decomposition of the PSC crystal structure.^[42,43] To better understand the kinetic Pb leaching behavior of PSCs, both static immersion and dynamic spraying experiments were performed. The experimental design of Pb leaching evaluation is illustrated in **Figure 1**, covering the experimental steps of: 1) PSC fabrication; 2) static soaking in acid and dynamic rainfall exposure as driving forces for Pb leaching; 3) pretreatment for dissolution of precipitates; and 4) quantitative Pb leaching analysis with inductively coupled plasma mass spectrometry (ICP–MS). The size of all PSC samples used for our study was 2.5×2.5 cm (length \times width). To allow for a straightforward analysis of the intrinsic Pb leaching behavior, we focus on analysis of PSCs without encapsulation, which is relevant to more extreme environmental scenarios where the device encapsulation fails or the devices are subjected to catastrophic physical damage.

We selected five types of high-performance PSCs with similar device architectures, namely, MAPbI₃, FAMA, FAMACs, CsPbI₃, and CsPbI₂Br, which are representatives of state-of-the-art organic–inorganic hybrid and inorganic PSCs.^[44–48] These benchmark high-performance PSCs were fabricated following recipes reported in the literatures,^[44–48] with their device parameters summarized in **Table 1**. *J*–*V* characteristics of the five types of PSCs under AM 1.5G (100 mW cm^{−2}) are shown in Figure S1, Supporting Information. The corresponding surface scanning electron microscope (SEM) images and X-ray diffraction patterns of the perovskite films are also shown in Figure S2 and S4, Supporting Information, respectively.

Since the processing method and antisolvents used are similar among all types of PSCs, the different amount of Pb measured is most likely attributed to the different thickness of the perovskite films, which has been optimized to obtain the best device efficiency for each kind of PSC. As shown in the cross-sectional SEM images in Figure S3, Supporting Information, the thickness of MAPbI₃, CsPbI₃, and CsPbI₂Br-based PSCs is in the range of 420 ± 30 nm, while the thickness of FA_{0.95}MA_{0.05}Pb(I_{0.95}Br_{0.05}) and Cs_{0.05}(FA_{0.85}MA_{0.15})_{0.95}Pb(I_{0.85}Br_{0.15})₃-based PSCs is in the range of 900 ± 30 nm. The total Pb amount measured is therefore closely correlated to the thickness of the perovskite layers. Beyond film thickness, other factors such as the density of the perovskite films and residual PbI₂ during perovskite

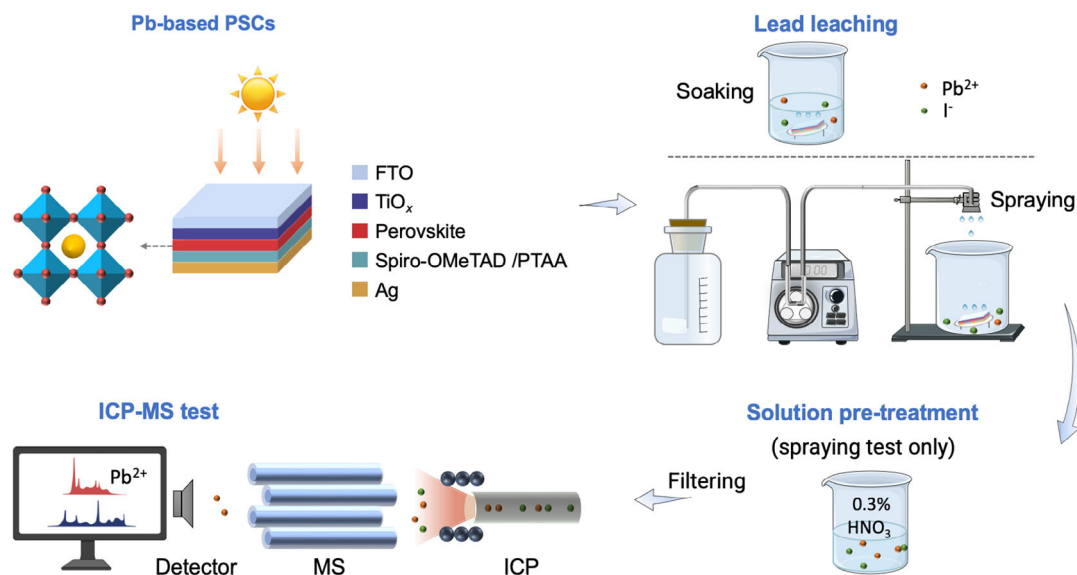


Figure 1. Schematic experimental procedures of Pb leaching evaluation.

Table 1. Device structures and parameters of PSCs were measured under AM 1.5G (100 mW cm^{−2}), room temperature (25 °C), and ambient moisture condition.

PSCs	Device structure	<i>J</i> _{sc} [mA cm ^{−2}]	<i>V</i> _{oc} [V]	FF	PCE [%]	PCE [%] in refs
MAPbI ₃	FTO/TiO ₂ /MAPbI ₃ /Spiro-OMeTAD/Ag	22.69	1.10	0.77	19.22	17.80 ^[44]
FAMA	FTO/TiO ₂ /FA _{0.95} MA _{0.05} Pb(I _{0.95} Br _{0.05}) ₃ /Spiro-OMeTAD/Ag	22.90	1.09	0.76	18.97	19.18 ^[45]
FAMACs	FTO/SnO ₂ /(Cs _{0.05} (FA _{0.85} MA _{0.15}) _{0.95} Pb(I _{0.85} Br _{0.15}) ₃ /Spiro-OMeTAD/Ag	22.69	1.09	0.78	19.30	19.00 ^[46]
CsPbI ₃	FTO/TiO ₂ /CsPbI ₃ /Spiro-OMeTAD/Ag	22.87	1.09	0.76	18.94	17.06 ^[47]
CsPbI ₂ Br	FTO/TiO ₂ /CsPbI ₂ Br/Spiro-OMeTAD/Ag	16.33	1.14	0.80	14.89	13.27 ^[48]

formation might also play a role in the different amount of Pb measured.

It is reported that PbI_2 or PbBr_2 is among the major decomposition product of perovskite materials, which only have modest solubility in pure water.^[42,49] For accurate determination of the total amount of Pb leached, different concentrations of sodium thiosulfate (0.05, 0.1, 0.2, 0.5, 50 mL) and nitric acid (0.3%, 1%, 3%, 50 mL) were selected as eluents to transform any precipitates into soluble ions, as shown in Figure S5, Supporting Information. As shown in Figure S6a,b, Supporting Information, at least 0.1 mol L^{-1} sodium thiosulfate is required to obtain a dissolution rate over 90%, while the high sodium thiosulfate concentration may lead to pipe blocking and instrument corrosion. In comparison, 0.3% nitric acid is sufficient to dissolve all precipitates (Figure S6b, Supporting Information), which was therefore selected throughout the study for the pretreatment of all extracted solutions.

Static soaking tests were first conducted to determine the total amount of Pb contained in each type of PSC. Unencapsulated PSC samples were submerged in 30 mL of 0.3% nitric acid (by volume) for 1, 5, or 10 days. The Pb leaching amount per unit area L_{total} is given by

$$L_{\text{total}} = \frac{c}{V \times S_{\text{PSC}}} \quad (1)$$

where c denotes the Pb density measured by ICP-MS, V denotes the volume of the pretreated solution, and S_{PSC} denotes the effective area of PSCs. The total amount of Pb contained in the PSCs is determined by the accumulated Pb leaching amount after 10 days of soaking. PSCs were found to lose all the color, indicating that all the precipitates were fully dissolved. After 10 days of static soaking, the total Pb leaching amount of MAPbI_3 -, FAMA-, FAMACs-, CsPbI_3 -, and CsPbI_2Br -based PSCs was calculated to be 438.26, 917.50, 943.45, 439.77, and 493.54 mg m^{-2} respectively (Figure 2). The Pb leaching amount after different days of static soaking is divided by the total Pb amount to obtain the quantitative leaching percentage. CsPbI_3 -based PSCs leached 99.1% of total amount of Pb after 1 day of soaking, further increasing to 99.7% after 5 days of soaking, the fastest in the percentage of Pb leaching. In comparison, FAMA-based PSCs

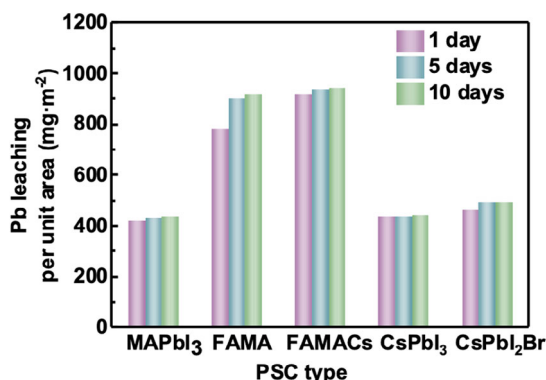


Figure 2. Pb leaching from five different types of PSCs (namely MAPbI_3 , $\text{FA}_{0.95}\text{MA}_{0.05}\text{Pb}(\text{I}_{0.95}\text{Br}_{0.05})_3$, $\text{CS}_{0.05}(\text{FA}_{0.85}\text{MA}_{0.15})_{0.95}\text{Pb}(\text{I}_{0.85}\text{Br}_{0.15})_3$, CsPbI_3 , and CsPbI_2Br) after immersion in 30 mL of 0.3% nitric acid separately for 1, 5, and 10 days.

leached 85.5% of total amount of Pb after 1 day of soaking, increasing to 98.5% after 5 days of soaking, the slowest in the percentage of Pb leaching. MAPbI_3 -, FAMA-, and CsPbI_2Br -based PSCs leached 96.3%, 97.4%, and 93.4% of total Pb amount after 1 day of soaking, increasing to 98.9%, 99.7%, and 99.5% after 5 days of soaking, respectively. It is obvious that all types of PSCs suffer from almost complete leaching of Pb within the first day of static soaking (see further details in Table S1, Supporting Information).

We further extend our studies to Pb leaching analysis under dynamic laboratory rainfall conditions, which is relevant to real-life conditions. The amount of Pb leached from unencapsulated PSCs under rainfall (freshwater) exposure is shown in Figure 3a. The initial Pb leaching dynamics can be revealed by varying the duration of rainfall spray at 10, 30, 60, 120, 240, 480, and 960 s. The absolute amount of Pb leaching after 960 s of spray time is strongly correlated to the total amount of Pb in the PSCs, with CsPbI_3 -based PSCs exhibiting the least amount of Pb leaching and FAMA-based PSCs exhibiting the most. This result suggests that liquid water can easily infiltrate throughout the whole perovskite film, causing strong tendency for Pb leaching upon aqueous exposure across all types of PSCs investigated, thereby resulting in a strong dependence of the Pb leaching rate upon the total amount of Pb contained in the PSCs. The leakage ratio/percentage can be calculated with L_i/L_{total} , where L_{total} is the total amount of Pb in the PSCs determined in the static soaking test. As shown in Figure 3b, CsPbI_2Br -based PSCs leached 97.3% of total amount of Pb after 960 s of rainfall exposure, compared with 91.2%, 91.8%, 60.4%, and 84.9% for MAPbI_3 -, FAMA-, FAMACs-, and CsPbI_3 -based PSCs, respectively. Surprisingly, over 60% of total Pb amount was leached within the first 120 s of rainfall exposure for all types of PSCs investigated, demonstrating that the leaching of Pb in aqueous environments can be extremely fast, with most of the Pb in the PSCs leached from unencapsulated devices within a timescale from seconds to minutes.

However, it should be noted that the Pb leaching rate (especially within the first 120s of rainfall exposure) appears to be strongly dependent on the types of PSCs studied, as shown in Figure 3b's inset. It is thus plausible that the different material compositions, crystal structures, film quality, and/or crystal stability of PSCs could have a strong impact upon Pb leaching. First, the moisture stability of the perovskite crystal structure appears to play a major role in the initial Pb leaching rate of PSCs. It has been reported that while all-inorganic CsPbI_3 - and CsPbI_2Br -based PSCs are considered to have greater thermal stability than organic-inorganic PSCs, they are known to be more sensitive to moisture, which accelerates the phase degradation of α -phase to the nonperovskite δ -phase.^[50,51] As shown in Figure 3b, it's apparent that CsPbI_3 and CsPbI_2Br -based PSCs exhibit higher initial Pb leaching rates within the first 60 s than other types of PSCs. This result suggests that moisture-induced crystal decomposition may serve as the first step for Pb leaching upon aqueous exposure. It has been reported that the original perovskite film could rapidly decompose into solid $\text{PbI}_2/\text{PbBr}_2$ precipitates as well as water-soluble byproducts within seconds of exposure to water.^[49,52] After 60 s, we observe a steady increase in the Pb leaching amount for FAMA- and FAMACs- based PSCs, which contain a higher total amount of Pb than the other types of PSCs. This results suggest that the total Pb amount contained in the perovskite film also plays a significant role, especially in the longer

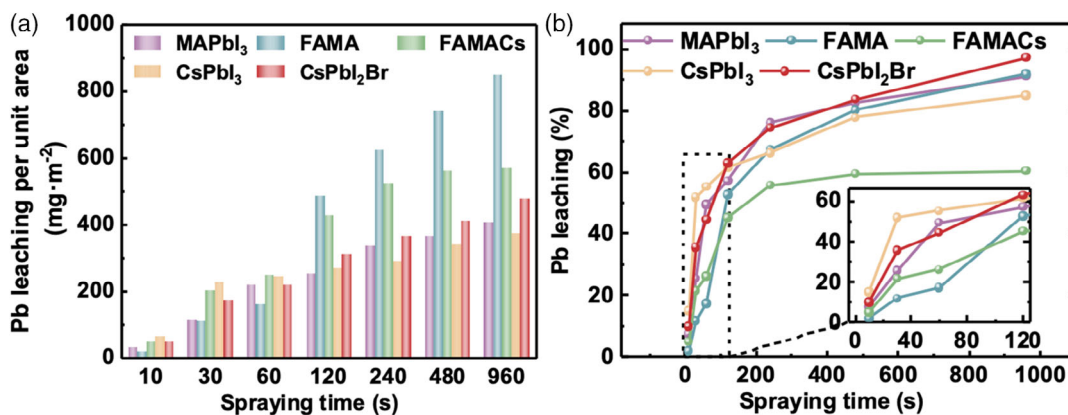


Figure 3. Pb leaching dynamics of the five different types of PSCs under pure water rainfall exposure. a) Pb leaching per unit area from 0 to 960 s. b) Pb leaching percentage at 0–960 s intervals and inset is 0–120 s intervals.

term (>60 s). In addition, film quality also appears to play an important role in the Pb leaching kinetics. For example, for the organic–inorganic PSCs (MAPbI₃, FA_{0.95}MA_{0.05}Pb(I_{0.95}Br_{0.05}), and Cs_{0.05}(FA_{0.85}MA_{0.15})_{0.95}Pb(I_{0.85}Br_{0.15})₃), films with bigger grain size and less grain boundaries (e.g., FA_{0.95}MA_{0.05}Pb(I_{0.95}Br_{0.05})₃) generally have a lower Pb leaching rate than films with smaller grain size and more grain boundaries (e.g., MAPbI₃, Cs_{0.05}(FA_{0.85}MA_{0.15})_{0.95}Pb(I_{0.85}Br_{0.15})₃). It is known that defects at grain boundaries and interfaces can serve as infiltration channels and initiate irreversible degradation of the perovskite film.^[52] It thus appears that the Pb leaching kinetics is a complicated process, which is a result of multiple competing factors. While more systematic experiments are needed to fully unravel the Pb leaching mechanisms and deconvolute the effects of individual factors, our findings point to a potential route to achieving significant Pb leaching reduction through further optimization of the materials design of PSCs.

We further investigate the effect of pH and temperature, two major environmental parameters, upon Pb leaching. Considering that soil environments can cover a broader pH range in real life, we compare the Pb leaching rate across a wider pH range of 1–9. The pH of rainwater was adjusted to 1, 3, 5, 7, 9 with 0.1 M hydrochloric acid and 0.1 M sodium hydroxide. **Figure 4a,b** shows the quantity and percentage of Pb leaching upon rainfall exposure of different pH for 60 s. Whilst the variation in Pb leaching rate is found to be insignificant across the pH range of 5–7 (commensurate to typical rainwater conditions), a higher leaching rate is observed at lower (<5) and higher (>7) pH levels, consistent with previous report.^[53] It has been reported that Pb compounds are generally more soluble at low soil pH (pH < 5).^[54] It is therefore plausible that the pH-dependent Pb leaching rate is related to the increased solubility and metal mobility in acidic eluents.^[55] This is consistent with our findings, where the most severe Pb leaching occurs at pH = 1 for all types of PSCs. In alkaline conditions, a slightly higher-than-average amount of Pb leaching was also observed. The hydroxide ions and hydroxyl radicals are known to be associated in a variety of perovskite surface chemical reactions, possibly promoting the desorption process.^[53,56] It is therefore likely that the pH-dependent Pb leaching rate is attributed to the accelerated

decomposition reaction of the perovskite materials in the presence of hydrogen ions and hydroxide ions.^[53]

We further investigate the effect of temperature upon the Pb leaching behavior. The temperature of the rainwater was varied at 10, 20, 30, and 40 °C, covering a temperature range commensurate to typical real-life conditions. As illustrated in Figure 4c,d, the amount of Pb leaching upon 60 s of rainfall exposure does not differ significantly over the temperature range, indicating general insensitivity of Pb leaching to temperature.

The results above demonstrate that Pb, a major hazardous substance of PSCs, can easily leak out of PSCs under aqueous exposure. The leached Pb can subsequently migrate within the environment and uptake by other living organisms, resulting in potentially significant environmental and ecotoxicological impacts. As a considerable amount of Pb was found to leach out of PSCs, their potential environmental risks were evaluated. If damaged PSCs are discarded, the increment amount of Pb leaching into the soil L_i can be calculated with the equation^[40]

$$L_i = \frac{c \times S_{\text{PSC}}}{V_{\text{soil}} \times \rho_{\text{soil}}} \quad (2)$$

where c denotes the amount of Pb leaching per unit area and V_{soil} denotes the soil volume. The dry bulk density of soil is denoted as ρ_{soil} , and the average value is 1.3 g cm^{-3} .^[57] If 1000 m^2 PSC modules are constructed during a large-scale ground installation and 80% of soil area is covered, the effective size of PSCs, S_{PSC} , is assumed to be 800 m^2 . It was asserted that the Pb species formed during perovskite decomposition by rain would strongly adsorb on soil particles, remaining concentrated in the top few centimeters, resulting in a greater Pb concentration near the soil surface.^[36] In this case, we assumed that Pb penetrated the soil 1 cm below the surface, since Pb tends to be highly absorbed by soil particles. The maximum Pb concentration in the polluted soil is calculated to rise by 43.5 mg kg^{-1} . The standard Pb concentration of uncontaminated soil ranges from 10 to 50 mg kg^{-1} , while urban soils often have much greater Pb concentrations, typically above 150 mg kg^{-1} .^[58] While this level of leaching appears below the limit, we need to note that very little is known about the exact chemical and

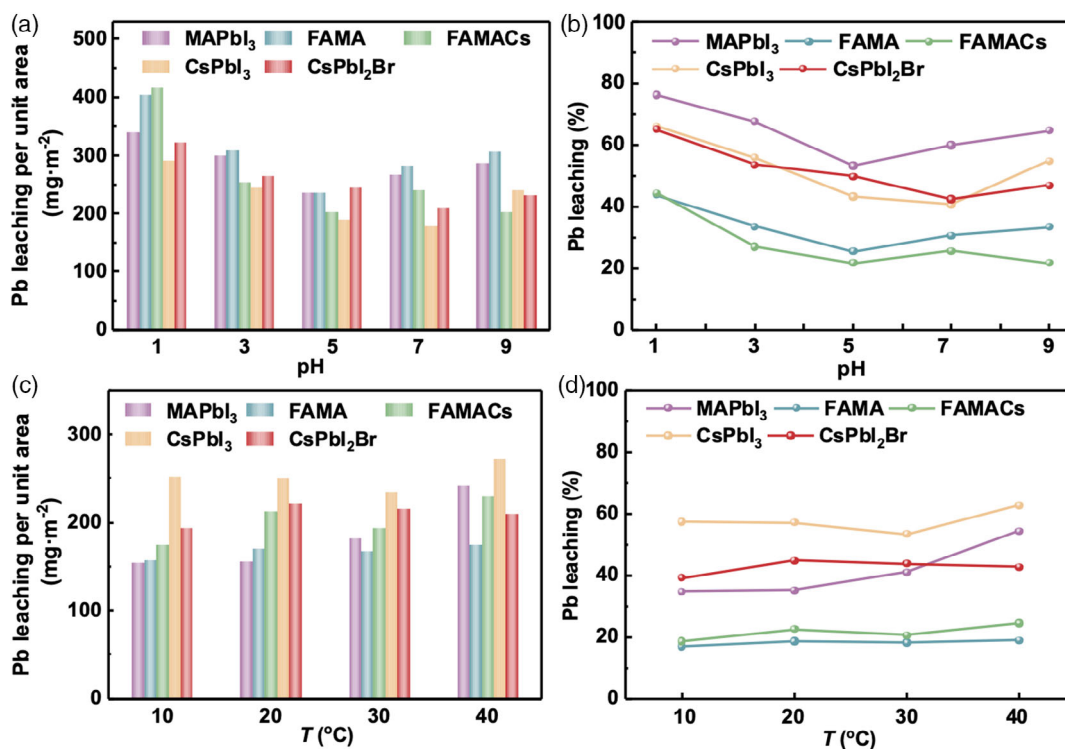


Figure 4. Pb leaching ratio of PSCs with simulated rainfall spraying for 60 s under various pH values and temperatures. a) Pb leaching per unit area in solutions with varying pH. b) Pb leakage percentage in solutions with different pH values. c) Pb leaching per unit area at different temperatures. d) Pb leakage percentage at different temperatures.

structural properties of the leachates as well as their solubility and environmental mobility, which could have a significant impact on their ecotoxicity. Moreover, Pb does not biodegrade or vanish over time, but rather persists for thousands of years in soils.^[54,58] For indoor photovoltaic applications or wearable electronics, human exposure to Pb through skin contact or inhalation is highly likely. Therefore, it is necessary to recognize that other possible sources of Pb exposure exist to cumulate, such as home interiors or school or daycare playgrounds. Finally, it's worth mentioning that Pb leaching of PSCs is on a similar level to solar cells based on PbS QDs, another class of emerging indoor PV technology^[59,60] (Figure S7, Supporting Information), suggesting that mitigating the environmental risks caused by Pb leaching can be a general critical challenge toward the commercialization of multiple technologies based on emerging Pb-based semiconductors.

3. Conclusion

We performed a quantitative analysis of the Pb leaching dynamics of five types of state-of-the-art PSCs. We found that significant Pb leaching could occur rapidly, with more than 60% of total amount of Pb found to leach from the PSCs within the first 120 s upon aqueous exposure. Our results suggest that the Pb leaching process of PSCs in aqueous environments could be a complicated process mediated by multiple competing factors, including in particular 1) the moisture stability of the perovskite

crystal structure, with crystal decomposition serving as the first step for Pb leaching; 2) film quality, with grain boundaries and other defects facilitating water infiltration; and 3) the total Pb amount contained in the perovskite film contributing to Pb leaching in the longer term. Our results provide quantitative and kinetic insights for the environmental impact assessment, materials screening, and encapsulation and packaging of PSCs, highlighting the importance of incorporating effective mitigation methods to minimize Pb leaching toward their large-scale commercialization.

4. Experimental Section

Materials: Methylammonium iodide (MAI, 99.5%), Lead iodide (PbI₂, 99.99%), Lead(II) Bromide (PbBr₂, 99.99%), Cesium iodide (CsI, 99.9%), Spiro-OMeTAD (99.8%), 4-*tert*-butylpyridine (tBP, 99%), and lithium bis(trifluoromethanesulfonyl)imide (LiTFSI, 96%) were purchased from Xi'an Polymer Light Technology Corp. Methylammonium bromide (MABr, 99%) and formamidinium iodide (FAI, 99%) were purchased from Greatcell Solar Materials Pty Ltd. Titanium tetrachloride (TiCl₄), *N,N*-dimethylformamide (DMF, 99.9%), dimethyl sulfoxide (DMSO, 99.9%), isopropanol (IPA, 99.5%), chlorobenzene (CB, 99.8%), and acetonitrile (99.8%) were purchased from Sigma-Aldrich. 15% SnO₂ colloidal solution was purchased from Alfa Aesar. The lead standard solution (1000 mg L⁻¹ ± 0.3%) was purchased from o2si smart solutions (Charleston, USA). Rhenium Standard Solution (50 µg L⁻¹) was obtained from Guobiao (Beijing) Testing & Certification Co., Ltd. (Beijing, China). Sodium thiosulfate was purchased from Tianjin Kermel Chemical Reagent Co., Ltd. (Tianjin, China). Nitric acid (68%) was produced from Guangzhou Chemical Reagent Factory (Guangzhou, China). Nylon filter

(0.45 μm) was purchased from Tianjin Jinteng Experimental Equipment Co., Ltd. (Tianjin, China). All chemicals were used as received without further purification.

Electron Transport Layer (ETL) Solution Preparation: 3% SnO_2 electron transport layer (ETL) colloidal solution was prepared by diluting 15% SnO_2 colloidal solution in deionized water and then ultrasound for 10 min. Then, the SnO_2 ETL solution was deposited on cleaned FTO-coated glass at 3000 rpm for 40 s and annealed at 150 $^\circ\text{C}$ for 30 min. Then, the SnO_2 ETL solution was deposited on the cleaned FTO-coated glass at 3000 rpm for 40 s and annealed at 150 $^\circ\text{C}$ for 30 min. The TiO_2 ETL was prepared by immersing the substrates in 200 mL of TiCl_4 solution at 70 $^\circ\text{C}$ for 1 h.

Perovskite Solution Preparation: The MAPbI_3 precursor solution was prepared by dissolving 461.01 mg PbI_2 and 157.96 mg MAI in 1 mL γ -butyrolactone and DMSO mixture solvent (7:3 v/v). The $\text{FA}_{0.95}\text{MA}_{0.05}\text{Pb}(\text{I}_{0.95}\text{Br}_{0.05})_3$ precursor solution was prepared by dissolving 645.50 mg PbI_2 , 240.76 mg FAI, 25.09 mg PbBr_2 , and 7.62 mg MABr, in 1 mL *N,N*-dimethyl formamide/dimethyl sulfoxide (4:1 v/v) mixed solvent. The $\text{Cs}_{0.05}(\text{FA}_{0.85}\text{MA}_{0.15})_{0.95}\text{Pb}(\text{I}_{0.85}\text{Br}_{0.15})_3$ precursor solution was prepared by dissolving 599.00 mg PbI_2 , 223.00 mg FAI, 73.40 mg PbBr_2 , 77.00 mg MABr, and 19.48 mg CsI in a mixture solvent of DMF and DMSO (4:1 v/v). The CsPbI_3 precursor solution was prepared by dissolving 259.00 mg DMAI, 461.00 mg PbI_2 , and 156.00 mg CsI_2 in DMSO solvent. The CsPbI_2Br precursor solution was prepared by dissolving 138.00 mg CsI_2 , 246.00 mg PbI_2 , 98.00 mg PbBr_2 , and 57.00 mg CsBr_2 in DMSO.

Spiro-OMeTAD Solution Preparation: After dissolving 90 mg Spiro-OMeTAD powder in 1 mL CB, 36 μL tBP and 22.5 μL Li-TFSI (520 mg mL^{-1} in acetonitrile) were added.

Devices Fabrication: The MAPbI_3 precursor solution was spin coated on the TiO_2 ETL for 40 s (4000 rpm, 2000 rpm s^{-1}), treated with 200 μL CB by drop casting at 20 s, and then annealed at 100 $^\circ\text{C}$ for 10 min. Subsequently, the 100 μL spiro-OMeTAD solution was spin coated on the perovskite film for 30 s (5000 rpm, 2000 rpm s^{-1}). After that, the 10 nm MoO_3 (0.03–0.05 nm s^{-1}) and 100 nm Ag (0.2 nm s^{-1}) were deposited. The similar fabrication steps were employed by other PSCs except the following perovskite film preparation process.

The $\text{FA}_{0.95}\text{MA}_{0.05}\text{Pb}(\text{I}_{0.95}\text{Br}_{0.05})_3$ precursor solution was spin coated on TiO_2 ETL at 1000 rpm for 10 s and then 5000 rpm for 20 s. It was treated with 200 μL CB by drop casting at 20 s and then 100 $^\circ\text{C}$ annealed for 10 min.

The $\text{Cs}_{0.05}(\text{FA}_{0.85}\text{MA}_{0.15})_{0.95}\text{Pb}(\text{I}_{0.85}\text{Br}_{0.15})_3$ precursor solution was spin coated on SnO_2 ETL at 1000 rpm for 10 s (1000 rpm s^{-1}) at 6000 rpm for 30 s (3000 rpm s^{-1}) and treated with 200 μL CB at 25 s. It was then 100 $^\circ\text{C}$ annealed for 10 min.

The CsPbI_3 precursor solution was spin coated on 90 $^\circ\text{C}$ TiO_2 ETL at 4000 rpm for 40 s, treated with 200 μL CB drop cast at 20 s, and then 210 $^\circ\text{C}$ annealed for 5 min.

The CsPbI_2Br was spin coated on 90 $^\circ\text{C}$ TiO_2 ETL at 1000 rpm for 10 s (1000 rpm s^{-1}) and then 3000 rpm for 30 s (2000 rpm s^{-1}), treated with 200 μL CB drop cast for 30 s and then 260 $^\circ\text{C}$ annealed for 10 min.

Solution Pretreatment: Nitric acid was added to the solutions after static soaking or dynamic spraying to achieve a 0.3% concentration. The mixed solution was left still for 24 h, then sonicated for 2 h, and at last left still for 12 h. Furthermore, solutions were filtered with a 0.45 μm nylon filter and then diluted for the ICP–MS test.

Spraying Test Setup: Dynamic rain spraying was simulated with ultra-pure water delivered via a peristaltic pump (Longer WT600-2)). The device was attached to a bracket at a 30 $^\circ$ angle to simulate the installation situation for solar cells.

ICP–MS Test: Pb concentration was measured by ICP–MS (NexION 300, Perkin Elmer), with rhenium (50 $\mu\text{g L}^{-1}$) as the internal standard. 10 mg L^{-1} Pb standard solution was prepared by diluting 1 mL 1000 mg L^{-1} Pb standard solution in a 100 mL volumetric flask with ultrapure water. Then, it was further diluted stepwise to 0, 1, 5, 10, 50, 100, and 300 $\mu\text{g L}^{-1}$ to get the standard curve before testing. During the ICP–MS test, KED mode was used, and the gas flow was 3.5 L min^{-1} . All results reported were repeated with at least three different samples.

Supporting Information

Supporting Information is available from the Wiley Online Library or from the author.

Acknowledgements

D.Y. and X.L. contributed equally to this work. This research was supported by the National Natural Science Foundation of China (22106021 and 61704027), the Guangdong Basic and Applied Basic Research Foundation (2021A1515012372), Research Fund of Guangdong-Hong Kong-Macao Joint Laboratory for Intelligent Micro-Nano Optoelectronic Technology (no. 2020B1212030010), and Engineering and Physical Sciences Research Council (EPSRC, EP/V039717/1) and Royal Society of Chemistry (E21-9668828170).

Conflict of Interest

The authors declare no conflict of interest.

Data Availability Statement

The data that support the findings of this study are available from the corresponding author upon reasonable request.

Keywords

indoor photovoltaics, kinetic studies, lead leaching, perovskite solar cells, quantum dots

Received: April 14, 2022

Revised: June 3, 2022

Published online:

- [1] G. E. Eperon, S. D. Stranks, C. Menelaou, M. B. Johnston, L. M. Herz, H. J. Snaith, *Energy Environ. Sci.* **2014**, 7, 982.
- [2] L. M. Herz, *ACS Energy Lett.* **2017**, 2, 1539.
- [3] W. Li, M. U. Rothmann, Y. Zhu, W. Chen, C. Yang, Y. Yuan, Y. Y. Choo, X. Wen, Y.-B. Cheng, U. Bach, J. Etheridge, *Nat. Energy* **2021**, 6, 624.
- [4] X. Du, J. Li, G. Niu, J. H. Yuan, K. H. Xue, M. Xia, W. Pan, X. Yang, B. Zhu, J. Tang, *Nat. Commun.* **2021**, 12, 3348.
- [5] C. Ashworth, *Nat. Rev. Mater.* **2021**, 6, 293.
- [6] P. Meredith, A. Armin, *Nat. Commun.* **2018**, 9, 5261.
- [7] J. J. Yoo, G. Seo, M. R. Chua, T. G. Park, Y. Lu, F. Rotermund, Y. K. Kim, C. S. Moon, N. J. Jeon, J. P. Correa-Baena, V. Bulovic, S. S. Shin, M. G. Bawendi, J. Seo, *Nature* **2021**, 590, 587.
- [8] J. Jeong, M. Kim, J. Seo, H. Lu, P. Ahlawat, A. Mishra, Y. Yang, M. A. Hope, F. T. Eickemeyer, M. Kim, Y. J. Yoon, I. W. Choi, B. P. Darwich, S. J. Choi, Y. Jo, J. H. Lee, B. Walker, S. M. Zakeeruddin, L. Emsley, U. Rothlisberger, A. Hagfeldt, D. S. Kim, M. Gratzel, J. Y. Kim, *Nature* **2021**, 592, 381.
- [9] G.-H. Kim, D. S. Kim, *Joule* **2021**, 5, 1033.
- [10] M. A. Green, S. P. Bremner, *Nat. Mater.* **2016**, 16, 23.
- [11] L. Qiu, L. K. Ono, Y. Qi, *Mater. Today Energy* **2018**, 7, 169.
- [12] H. Min, D. Y. Lee, J. Kim, G. Kim, K. S. Lee, J. Kim, M. J. Paik, Y. K. Kim, K. S. Kim, M. G. Kim, T. J. Shin, S. Il Seok, *Nature* **2021**, 598, 444.
- [13] A. Al-Ashouri, E. Köhnen, B. Li, A. Magomedov, H. Hempel, P. Caprioglio, J. A. Márquez, A. B. M. Vilches, E. Kasparavicius,

- J. A. Smith, N. Phung, D. Menzel, M. Grischek, L. Kegelman, D. Skroblin, C. Gollwitzer, T. Malinauskas, M. Jošt, G. Matič, B. Rech, R. Schlatmann, M. Topič, L. Korte, A. Abate, B. Stannowski, D. Neher, M. Stolterfoht, T. Unold, V. Getautis, S. Albrecht, *Science* **2020**, 370, 1300.
- [14] X. Hou, Y. Wang, H. K. H. Lee, R. Datt, N. Uslar Miano, D. Yan, M. Li, F. Zhu, B. Hou, W. C. Tsoi, Z. Li, *J. Mater. Chem. A* **2020**, 8, 21503.
- [15] B. Li, B. Hou, G. A. J. Amaratunga, *InfoMat* **2021**, 3, 445.
- [16] Y. T. Huang, S. R. Kavanagh, D. O. Scanlon, A. Walsh, R. L. Z. Hoye, *Nanotechnology* **2021**, 32, 132004.
- [17] A. Babayigit, A. Ethirajan, M. Muller, B. Conings, *Nat. Mater.* **2016**, 15, 247.
- [18] L. Gollino, T. Pauporté, *Sol. RRL* **2021**, 5, 2000616.
- [19] S. Attique, N. Ali, S. Rauf, S. Ali, A. Khesro, R. Khatoon, E. U. Khan, F. Akram, S. Yang, H. Wu, *Sol. RRL* **2021**, 5, 2100212.
- [20] F. Gu, Z. Zhao, C. Wang, H. Rao, B. Zhao, Z. Liu, Z. Bian, C. Huang, *Sol. RRL* **2019**, 3, 1900213.
- [21] A. Abate, *Joule* **2017**, 1, 659.
- [22] M. Li, Z. Wang, M. Zhuo, Y. Hu, K. Hu, Q. Ye, S. M. Jain, Y. Yang, X. Gao, L. Liao, *Adv. Mater.* **2018**, 30, e1800258.
- [23] M. Li, W. Zuo, Y. Yang, M. H. Aldamasy, Q. Wang, S. H. T. Cruz, S. Feng, M. Saliba, Z. Wang, A. Abate, *ACS Energy Lett.* **2020**, 5, 1923.
- [24] Y. Li, W. Sun, W. Yan, S. Ye, H. Rao, H. Peng, Z. Zhao, Z. Bian, Z. Liu, H. Zhou, C. Huang, *Adv. Energy Mater.* **2016**, 6, 1601353.
- [25] X. Lian, J. Chen, Y. Zhang, M. Qin, J. Li, S. Tian, W. Yang, X. Lu, G. Wu, H. Chen, *Adv. Funct. Mater.* **2019**, 29, 1807024.
- [26] S. Wu, Z. Li, M. Q. Li, Y. Diao, F. Lin, T. Liu, J. Zhang, P. Tieu, W. Gao, F. Qi, X. Pan, Z. Xu, Z. Zhu, A. K. Jen, *Nat. Nanotechnol.* **2020**, 15, 934.
- [27] Y. Jiang, L. Qiu, E. J. Juarez-Perez, L. K. Ono, Z. Hu, Z. Liu, Z. Wu, L. Meng, Q. Wang, Y. Qi, *Nat. Energy* **2019**, 4, 585.
- [28] X. Li, F. Zhang, H. He, J. J. Berry, K. Zhu, T. Xu, *Nature* **2020**, 578, 555.
- [29] X. Xiao, M. Wang, S. Chen, Y. Zhang, H. Gu, Y. Deng, G. Yang, C. Fei, B. Chen, Y. Lin, M. D. Dickey, J. Huang, *Sci. Adv.* **2021**, 7, eabi8249.
- [30] Z. Li, X. Wu, S. Wu, D. Gao, H. Dong, F. Huang, X. Hu, A. K. Y. Jen, Z. Zhu, *Nano Energy* **2022**, 93, 106853.
- [31] Y. Liang, P. Song, H. Tian, C. Tian, W. Tian, Z. Nan, Y. Cai, P. Yang, C. Sun, J. Chen, L. Xie, Q. Zhang, Z. Wei, *Adv. Funct. Mater.* **2022**, 32, 2110139.
- [32] J. Zhang, R. Li, S. Aperi, P. Wang, B. Shi, J. Jiang, N. Ren, W. Han, Q. Huang, G. Brocks, Y. Zhao, S. Tao, X. Zhang, *Sol. RRL* **2021**, 5, 2100464.
- [33] Y. G. Yoo, J. Park, H. N. Umh, S. Y. Lee, S. Bae, Y. H. Kim, S. E. Jerng, Y. Kim, J. Yi, *J. Ind. Eng. Chem.* **2019**, 70, 453.
- [34] G. Panthi, R. Bajagain, Y.-J. An, S.-W. Jeong, *Process Saf. Environ.* **2021**, 149, 115.
- [35] I. R. Benmessaoud, A. L. Mahul-Mellier, E. Horvath, B. Maco, M. Spina, H. A. Lashuel, L. Forro, *Toxicol. Res.* **2016**, 5, 407.
- [36] B. Hailegnaw, S. Kirmayer, E. Edri, G. Hodes, D. Cahen, *J. Phys. Chem. Lett.* **2015**, 6, 1543.
- [37] J. Li, H. L. Cao, W. B. Jiao, Q. Wang, M. Wei, I. Cantone, J. Lu, A. Abate, *Nat. Commun.* **2020**, 11, 310.
- [38] P. Su, Y. Liu, J. Zhang, C. Chen, B. Yang, C. Zhang, X. Zhao, *J. Phys. Chem. Lett.* **2020**, 11, 2812.
- [39] Y. Yu, Y. Hong, P. Gao, M. K. Nazeeruddin, *Anal. Chem.* **2016**, 88, 12316.
- [40] J. Wan, X. Yu, J. Zou, K. Li, L. Chen, Y. Peng, Y.-B. Cheng, *Sol. Energy* **2021**, 226, 85.
- [41] J. I. Kwak, L. Kim, T.-Y. Lee, G. Panthi, S.-W. Jeong, S. Han, H. Chae, Y.-J. An, *Aquat. Toxicol.* **2021**, 237, 105900.
- [42] E. Mosconi, J. M. Azpiroz, F. De Angelis, *Chem. Mater.* **2015**, 27, 4885.
- [43] S. Zhan, X.-B. Fan, J. Zhang, J. Yang, S. Y. Bang, S. D. Han, D.-W. Shin, S. Lee, H. W. Choi, X. Wang, B. Hou, L. G. Occhipinti, J. M. Kim, *J. Mater. Chem. C* **2020**, 8, 16001.
- [44] M. Li, Y. Yang, Z. Wang, T. Kang, Q. Wang, S. H. Turren-Cruz, X. Gao, C. Hsu, L. Liao, A. Abate, *Adv. Mater.* **2019**, 31, e1901519.
- [45] L. Wang, X. Wang, L. Zhu, S.-B. Leng, J. Liang, Y. Zheng, Z. Zhang, Z. Zhang, X. Liu, F. Liu, C.-C. Chen, *Chem. Eng. J.* **2022**, 430, 132730.
- [46] M. Li, W. Zuo, Q. Wang, K. Wang, M. Zhuo, H. Köbler, C. E. Halbig, S. Eigler, Y. Yang, X. Gao, Z. Wang, Y. Li, A. Abate, *Adv. Energy Mater.* **2019**, 10, 1902653.
- [47] Y. Wang, T. Zhang, M. Kan, Y. Zhao, *J. Am. Chem. Soc.* **2018**, 140, 12345.
- [48] K. Wang, X. Li, Y. Lou, M. Li, Z. Wang, *Sci. Bull.* **2021**, 66, 347.
- [49] Y.-Y. Zhang, S. Chen, P. Xu, H. Xiang, X.-G. Gong, A. Walsh, S.-H. Wei, *Chinese Phys. Lett.* **2018**, 35, 036104.
- [50] Y. Li, Y. Wang, T. Zhang, S. Yoriya, P. Kumnorkaew, S. Chen, X. Guo, Y. Zhao, *Chem. Commun.* **2018**, 54, 9809.
- [51] Y. Wang, X. Liu, T. Zhang, X. Wang, M. Kan, J. Shi, Y. Zhao, *Angew. Chem. Int. Ed. Engl.* **2019**, 58, 16691.
- [52] N. Ahn, K. Kwak, M. S. Jang, H. Yoon, B. Y. Lee, J. K. Lee, P. V. Pikhitsa, J. Byun, M. Choi, *Nat. Commun.* **2016**, 7, 13422.
- [53] L. Zhang, P. H. L. Sit, *J. Phys. Chem. C* **2015**, 119, 22370.
- [54] US EPA, *Lead in the Human Environment*, <https://www.epa.gov/lead/learn-about-lead#:~:text=Lead%20can%20be%20found%20in,lead%20based%20paint%20in%20homes> (accessed: May, 2022).
- [55] N. R. Brun, B. Wehrli, K. Fent, *Sci. Total Environ.* **2016**, 543, 703.
- [56] T. Schiros, L. Å. Näslund, K. Andersson, J. Gyllenpalm, G. S. Karlberg, M. Odelius, H. Ogasawara, L. G. M. Pettersson, A. Nilsson, *J. Phys. Chem. C* **2007**, 111, 15003.
- [57] R. K. Rai, V. P. Singh, A. Upadhyay, *Planning and Evaluation of Irrigation Projects*. Academic Press, Cambridge, MA, USA **2017**.
- [58] R. Stehouwer, K. Macneal, *Lead in Residential Soils: Sources, Testing, and Reducing Exposure*, <https://extension.psu.edu/lead-in-residential-soils-sources-testing-and-reducing-exposure>, (accessed: May, 2022).
- [59] B. Hou, B. S. Kim, H. K. H. Lee, Y. Cho, P. Giraud, M. Liu, J. Zhang, M. L. Davies, J. R. Durrant, W. C. Tsoi, Z. Li, S. D. Dimitrov, J. I. Sohn, S. Cha, J. M. Kim, *Adv. Funct. Mater.* **2020**, 30, 2004563.
- [60] D. Yan, M. Liu, Z. Li, B. Hou, *J. Mater. Chem. A* **2021**, 9, 15522.